Landscape evolution in flood-a mathematical model

1993 J. Phys. A: Math. Gen. 26 6777

(http://iopscience.iop.org/0305-4470/26/23/024)

J. Phys. A: Math. Gen. 26 (1993) 6777–6787. Printed in the UK

Landscape evolution in flood—a mathematical model

G N Barzini and R C Ball

Cavendish Laboratory, Madingley Road, Cambridge CB3 0HE, UK

Received 16 February 1993, in final form 19 August 1993

Abstract. We present analytical and numerical studies for the evolution of a landscape in flood. Our model is based on the assumption that the local fluxes of both water and sediment depend only (and simply) on the gradient of the water surface and local depth of flood. Nonlinear differential equations for water conservation dictate the distribution of flood-water. The divergence of the sediment flux then determines the net rise (deposition) or fall (erosion) of the underlying landscape. We present linear stability analysis for an initially planar slope, with uniform water flow: the dominant instability is the development of corrugations at an angle oblique to the flow direction. Numerical results are presented for the long time evolution of a system with periodic boundary conditions, and no net gain or loss of either water or sediment. The resulting landscape resembles that of a braided river bed, and analysis of the contours shows quantitative agreement with the experimental power law distribution of island sizes for the Zaire and Rakaia river systems and the outwash drainage system at Vatnajokull.

1. Introduction

Simulation of river flood-plains has tended to fall into three main categories:

(a) Models that incorporate a set of empirically determined equations to describe aspects of the flood-plain evolution [1]: these aim primarily at producing realistic flood-plain strata and less at determining variable interdependence.

(b) Detailed physical models which attempt to solve the fluid flow and sediment transport realistically [2]. These produce highly realistic results, but are limited to fairly small grids by the high computational cost. As with the first category, they tend to require detailed initial conditions and to exhibit a degree of complexity that can make understanding of individual aspects difficult.

(c) Simplistic physical models. These make important assumptions about the basic underlying processes such as water flow and erosion in order to gain simplicity at the expense of realism. While they were popular at a time when computer power was more limited, they were to some extent eclipsed as more detailed simulation became possible. There has however been a recent revival of interest in such models [3, 4] due to the comparative ease with which many features of their behaviour can be understood, and also to suggestions that some aspects of system behaviour may be comparatively independent of the details of the model. For example in [4] the authors found that the system as modelled exhibited self-organized criticality, a form of behaviour generally robust with respect to small changes of the model [5].

The model considered here falls into category (c); its purpose is to investigate how water flow over an initially flat plane of erodible sediment might lead to a non-uniform time evolution and to see what features might result from such a model: a central

0305-4470/93/236777+11$07.50

assumption is made that the evolution of the landscape itself is by far the slowest process involved, and thus that the water flow can be calculated, as a reasonable approximation, as though the landscape were static (there are clearly examples where this is inapplicable, but it has wide relevance to landscapes evolving over months or years). The water flow is then used to calculate the sediment transport, and hence the landscape evolution. In all cases the equations are made as simple as is consistent with elementary physical constraints.

2. Present model

Our model is based on the following principles and assumptions:

(i) The flow velocity is averaged vertically so as to have a single value $v(x, y)$ everywhere in the x–y plane.

(ii) The flow velocity is assumed to be a purely local function of slope and depth only, ensuring that the equations are purely differential in form, and simplifying the problem.

Given these assumptions a dimensional argument suggests that the velocity takes the form

$$v = -ad^{1/2} g_{\text{eff}} / (g_{\text{eff}})^{1/2} \tag{1}$$

where $d(x, y)$ is the water depth and a is some dimensionless constant depending on viscosity, density and coefficient of roughness. The effective gravitational acceleration acting on the water, g_{eff}, is taken as the component of gravity acting along the slope of the water surface. Assuming the slope to be shallow enough for small angle approximations to apply, one can therefore write:

$$g_{\text{eff}} = g\nabla(h + d) \tag{2}$$

where $h(x, y)$ is the height profile of the underlying land.

(iii) The water flux $\boldsymbol{q} = d\boldsymbol{v}$ is conserved:

$$\partial d/\partial t = -\nabla \cdot \boldsymbol{q}. \tag{3}$$

This completes our (simplistic) model of the water flow, in broad agreement with certain empirical models of dissipative water flow (see [2], chapter 4 and references therein).

Further assumptions are now needed about the erosion, transport and deposition. The complication here is that in reality a wide range of transport mechanisms are known to apply to different sediment types, and the relation between the rate of transport by these mechanisms and such factors as flow rate and degree of turbulence do not appear fully understood. The following simplifying assumptions were therefore used:

(iv) There is only one sediment type (clearly there are interesting generalizations if more sediment types are included, with interaction between them). The load (volume fraction) of sediment borne by the water will be denoted $L(x, y)$, and the flux of sediment will be assumed to be

$$\boldsymbol{q}_s = L\boldsymbol{q}. \tag{4}$$

(v) There is a maximum amount of sediment that the water can support at any given point, the capacity C, which can be described as a homogenous function of the depth and flow velocity:

$$C = Kd^{\alpha}v^{2\beta} \tag{5}$$

for some constants K, α, and β. Noting that C can readily be re-written as a function of any two not linearly related flow variables, this is again consistent with many of the empirical formulae describing sediment transport [2, 6].

(vi) Where there is a discrepancy between the load L and capacity C, sediment is eroded/deposited from the river bottom at a rate linear in the difference, with some time constant τ, leading to a rate of change in the landscape height, h, given by:

$$\partial h/\partial t = d(L-C)/\tau. \tag{6}$$

In general τ need not be a constant (it could include, for example, geometrical factors, although this is not considered further here), but is assumed to be the same for deposition and erosion, and also that the sediment has no cohesion: there is no flow threshold below which erosion cannot occur. This has no clear physical basis, it is adopted simply in order to make the rate of erosion/deposition an analytic function of the load/capacity imbalance. For these reasons we will go on to consider behaviour in the limit $\tau \to 0$.

(vii) Continuity of sediment

$$-\partial h/\partial t = \nabla \cdot (\boldsymbol{q}L) + d\,\partial L/\partial t \tag{7}$$

completes the model in principle.

(viii) In this paper the further simplifying assumption is made that the relaxation time of the water depth is negligible on the timescale over which the underlying terrain changes. Then for a given state of the landscape the water will effectively be in steady state and equation (3) is replaced by $\nabla \cdot \boldsymbol{q} = 0$.

3. Linear instability analysis

There is clearly a stationary solution of the model equations with constant slope, $h_0 = \boldsymbol{\theta} \cdot \boldsymbol{r}$ (or simply $h_0 = \theta x$), uniform depth d_0 and initially sediment-saturated: $L = C_0$. In such a set-up, with periodic boundary conditions, no net erosion or deposition occurs.

If a small perturbation of the bottom profile is introduced such that

$$h = h_0 + \Delta h = h_0 + h_1\,e^{i\boldsymbol{k}\cdot\boldsymbol{r}}$$

we can compute the resulting linear changes of depth and capacity,

$$\Delta d = A\Delta h \qquad \text{and} \qquad \Delta C = B\Delta h$$

in terms of (complex) amplitudes A and B.

Expanding $\boldsymbol{q}$ to first order in h_1 and imposing $\nabla \cdot \boldsymbol{q} = 0$ gives

$$A = -(1/2k_x^2 + k_y^2)/(1/2k_x^2 + k_y^2 - 3/2\theta i k_x/d_0) \tag{8}$$

and expanding C (from (5)) using this result for Δd gives

$$\begin{aligned} B &= -K(g\theta)^{\beta} d_0^{\alpha+\beta-1}\{\beta(ik_x(1+A)d_0/\theta + A) + \alpha A\} \\ &= K(g\theta)^{\beta} d_0^{\alpha+\beta-1}\{(\alpha+\beta)k_y^2 + (\alpha/2-\beta)k_x^2\}/(1/2k_x^2 + k_y^2 - 3/2\theta i k_x/d_0). \end{aligned} \tag{9}$$

Assuming that h_1 has time dependence e^{Pt}, equating (6) with (7) and rearranging gives

$$\Delta L = \Delta C/(d_0 + \tau(\mathrm{i}\boldsymbol{k}\cdot\boldsymbol{q} + pd_0)). \tag{10}$$

Substituting this back into (6) gives a quadratic in p with solutions

$$p_{\pm} = [-(d_0 + Bd_0^2 + \mathrm{i}\tau\boldsymbol{k}\cdot\boldsymbol{q}) \pm \{(d_0 + Bd_0^2 + \mathrm{i}\tau\boldsymbol{k}\cdot\boldsymbol{q})^2 - 4\mathrm{i}\tau\boldsymbol{k}\cdot\boldsymbol{q}Bd_0^2\}^{1/2}]/2d_0\tau.$$

The interesting root is p_+, the other, p_-, having a *-ve* real part over all plausible ranges of α, β (2–3 and 1.5–2 respectively) and so expected to have no significant effect on the behaviour of the system.

Figure 1 shows, $\mathrm{Re}(p_+)$ as a function of $\boldsymbol{k}$ in the plane. If $\boldsymbol{k}$ is written as $k(\cos\phi, \sin\phi)$ then $\mathrm{Re}(p_+) > 0$, giving exponential growth, for ϕ greater than a critical angle ϕ_c. Also, $\mathrm{Re}(p_+)$ has a maximum as a function of ϕ and tends to 0 as ϕ reaches $\pi/2$. This physically corresponds to the fact that this model conserves sediment: if there is no sink at the lower boundary, the only way for a channel to deepen is by there being a cross-channel component of water flow that transports sediment from troughs to crests. This clearly requires that $\boldsymbol{k}$ have a component parallel to $\boldsymbol{q}$, and hence, since $\boldsymbol{q}$ remains down-slope to zeroth order, channels running directly down-slope do not grow. (Growth could also be possible in principle by the increased flow down a channel, and hence increased capacity, outweighing the amount of sediment erosion needed to deepen the channel, but that does not apply here.)

4. Limiting cases

It can be seen in figure 1 that the angle of fastest growth, ϕ_m, tends to $\pi/2$ as k increases and examination of the equation show that this happens for $|\tau\boldsymbol{k}\cdot\boldsymbol{q}| \gg d_0$, where τ is an equilibration time for sediment load w.r.t. carrying capacity (equation (6)). This results from the fact that for significant deepening of a channel to occur, the time taken for sediment to be transported from a trough to a crest, given by $1/(\boldsymbol{k}\cdot\boldsymbol{v})$ must exceed τ, hence the angle between $\boldsymbol{k}$ and $\boldsymbol{v}$ increases with k. However, in a real system there must also be some competing cut-off at high k due to effects such as turbulent mixing, and the form of τ is also uncertain.

We are thus motivated to focus on the case where $\tau < 1/kv < 1/p$ holds, meaning physically that the time for sediment to be scoured/deposited is smaller than that for either the landscape or the water-flow to alter significantly. This has the advantages that the problem of an unknown and probably variable τ does not affect this regime, and the system no longer contains any timescale beyond that defined by the initial conditions (q/d_0^2). The rate of evolution simply scales with the size and slope of the system and the instability reduces to $p_+ = (-\mathrm{i}\boldsymbol{k}\cdot\boldsymbol{q}B)/(d_0 + d_0^2B)$.

One further approximation can be made that $|Bd_0| \ll 1$ in cases to which this model is applicable, equivalent to saying that $d\,\partial L/\partial t \ll \boldsymbol{q}\cdot\nabla L$, i.e. that the sediment load is in steady-state, which will be the case to first order in the rate of change of the terrain (which is small). Hence, p_+ becomes simply $-\mathrm{i}\boldsymbol{k}\cdot\boldsymbol{q}B/d_0$, with real part

$$3/2Kd_0^{\alpha+\beta-1/2}\theta^{\beta+3/2}g^{\beta+1/2}\frac{k^2\cos^2\phi((\alpha+\beta)\sin^2\phi + (\alpha/2-\beta)\cos^2\phi)}{[k^2(1/2\cos^2\phi + \sin^2\phi)^2 + 9/4\theta^2\cos^2\phi/d_0^2]} \tag{11}$$

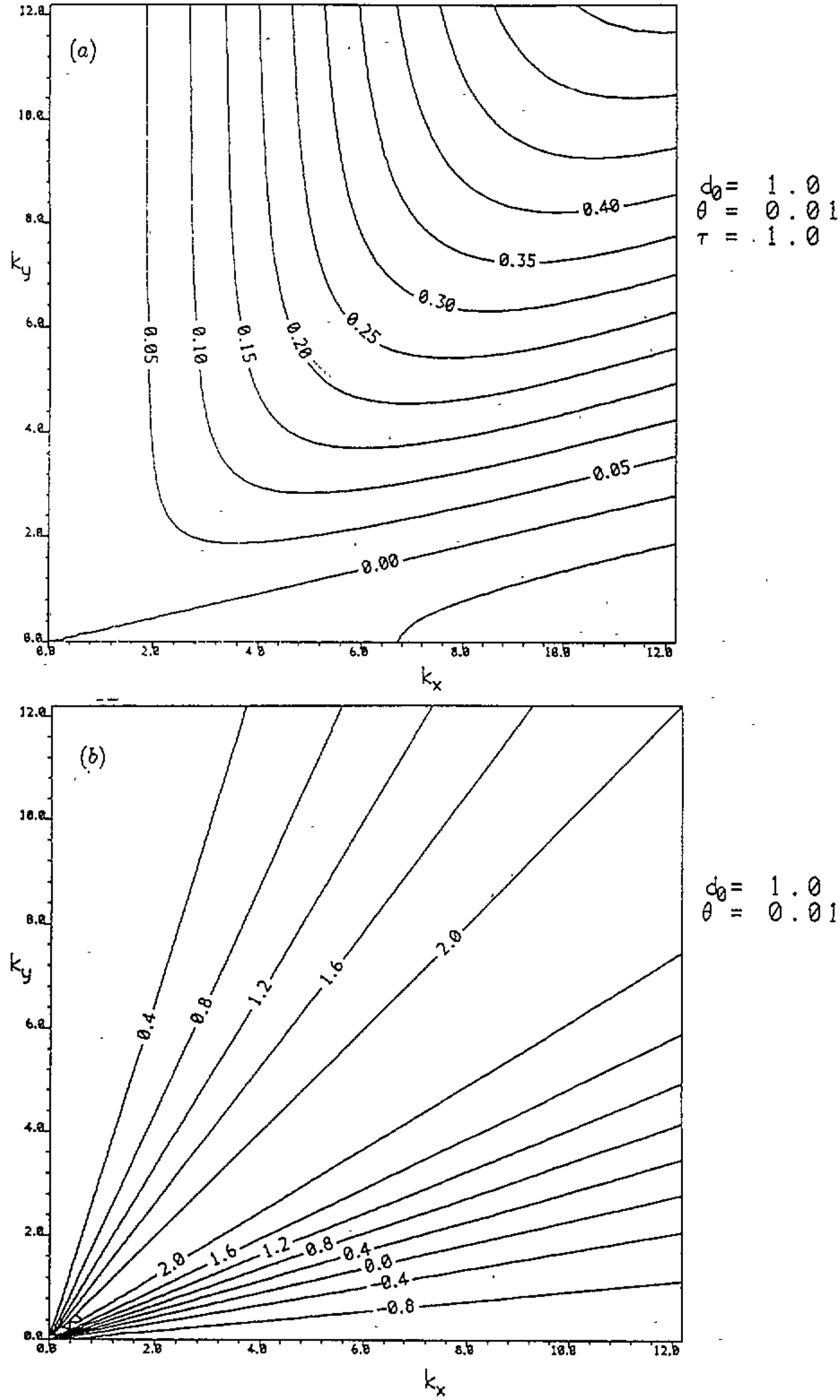

Figure 1. Contour plot of the real part of the growth exponent, $\mathrm{Re}(p_+)$, as a function of wavevector, $\boldsymbol{k}$, with $\alpha=3.0$, $\beta=1.75$, $K=1$: (*a*) the original form, (*b*) the limiting case of equation (11).

which clearly has a maximum at a definite value of ϕ (figure 1(b)) which is a function of α, β and k resulting in well defined channels at a definite angle to the downstream direction, the angle for the onset of instability being given by

$$\phi_c = \tan^{-1}[(\beta - \alpha/2)/(\beta + \alpha)]^{1/2}. \tag{12}$$

Also the angle of maximum growth no longer goes to $\pi/2$ as k increases.

There is also the k-dependence to consider. Here the main criterion is the value of k compared to θ/d. When significantly larger, the value of $\mathrm{Re}(p_+)$ reaches an asymptotic limit (approached significantly faster than in the case of $\tau = 1$), while for smaller values, it is quadratic in k resulting in behaviour that is diffusion-like or anti-diffusion-like depending on ϕ. While high wavenumber perturbations grow fastest, it seems possible that the length-scale d/θ plays a significant part in the behaviour of the system determining a length for large-scale structure.

5. Simulation

The nonlinear behaviour of the model has been explored by computer simulation, implementing the equations in their simplest form: low capacity so that water and sediment flow are at steady-state with the landscape, and negligible relaxation time of load to capacity (i.e. $\tau = 0$). The program (in standard FORTRAN77) uses a finite difference scheme, in both time and space, the spatial approximation being on a square lattice.

Progress in time is by an explicit forward-step method due to the difficulty of expressing the nonlinear equations in implicit form, although this limits the efficiency of the simulator, and a more sophisticated approach might ultimately be desirable.

In all cases the boundary conditions used were as follows: the initial condition was a uniform plane of sediment sloped in the x-direction to which a low level of white noise was added. The boundaries were effectively periodic in both directions: directly so along y, while along x allowance was made for the net drop across the grid, giving an arrangement in which the water flows continually downhill, returning to the same point (rather in the style of an M C Escher print).

Flow was calculated along the two bonds joining each lattice point to its nearest x and y neighbours. The gradient component along each bond being calculated by simple difference between the ends, while that across the bond was taken from the nearest neighbours to the bond end at right-angles to it (figure 2). The depth along the bond

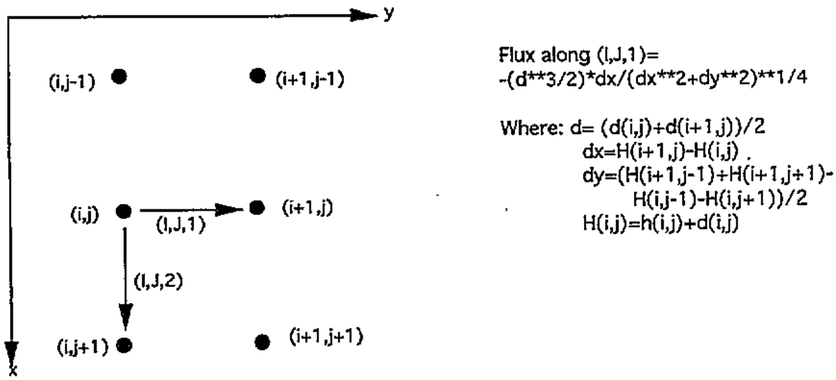

Figure 2. Diagram of difference scheme used in simulation.

was taken as the simple mean of the two end values†. Both the simulated solutions to the water flow problem alone and to sediment transport have been tested against the above analytic solutions in the limiting case of small sinusoidal perturbations: agreement is good, limited mainly by the grid-spacing.

6. Results and comparison

Perturbations at first grow exponentially, as suggested by the stability analysis. Once the features formed have reached a significant fraction of water depth, the rate of evolution peaks and then falls, eventually reaching a plateau level, several orders of magnitude lower than the peak, which exhibits noise of a partly power-law form (the power spectrum has a large low-frequency part, followed by a section that is to a good approximation power-law with exponent -2). This plateau behaviour then persists, corresponding to a statistical steady state in which some features fade while others appear and at the same time there is a gradual overall dispersion upstream (while not immediately intuitive, this is not necessarily inconsistent with real systems). A typical result is shown in figure 3(a). The principal features are sets of ridges and troughs, of

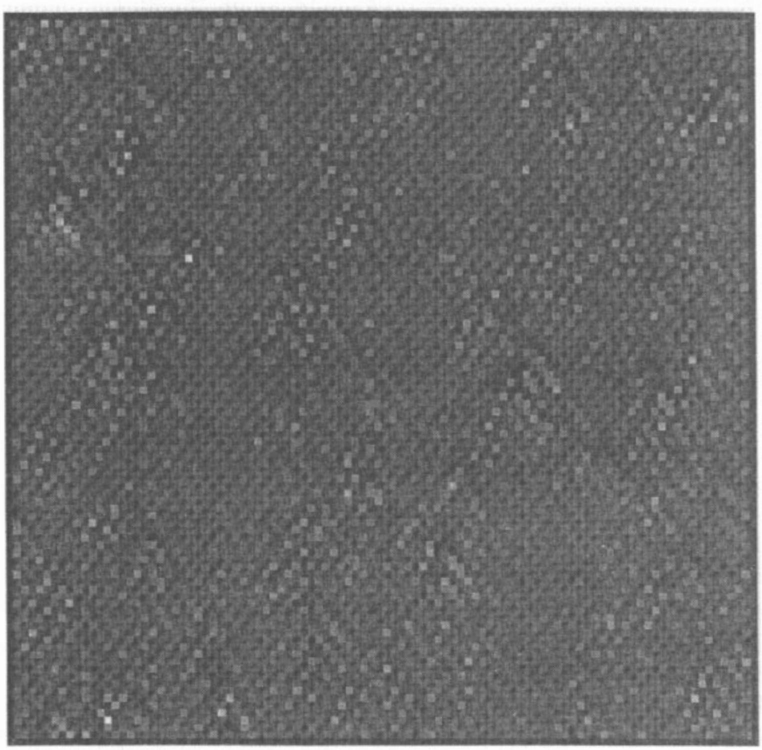

Figure 3a. Plot of results from a simulation on a 100×100 grid with: $\alpha = 3.0$, $\beta = 1.75$, $d_0 = 0.1$ (where the grid-spacing $= 1.0$) and $\theta = 0.02$. The top of the page corresponds to the top of the slope. Inverted V-shaped patterns of disturbance can be seen on a smoother background (light correspond to higher ground, dark to lower, the background slope has been subtracted off to increase the visibility of these features).

† Other averaging schemes for the depth such as the harmonic mean are being considered in current work.

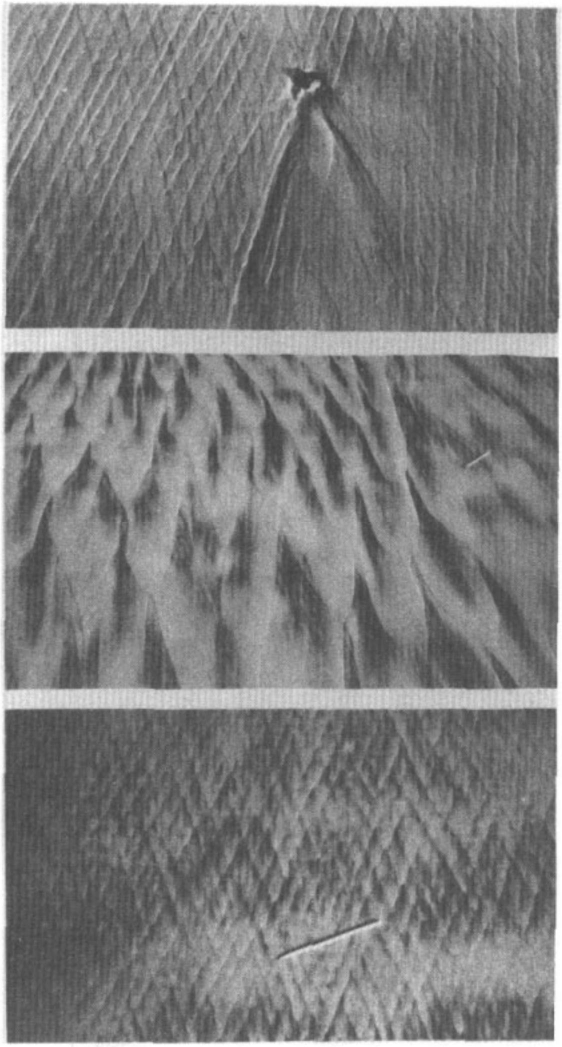

Figure 3b. Examples of rhomboid rill patterns (from [7]).

wavelength about two lattice-spacings, which run at a clear preferred angle to the downstream direction. This is in line with the results of the stability analysis, although variations (e.g. adapting the simulation to a triangular grid) show that the angle is affected by the lattice vectors of the grid. There is also a definite division on a larger scale into strongly and weakly ridged regions.

Visually there is a noticeable resemblance to features left on beaches by outgoing tides, known as rhomboid rills (figure 3(*b*)) [7]. This may be explained by the fact that these features are formed on a surface of sand initially approximately flat, by flow of a small depth of water for a comparatively short time, so that the effect of the open boundaries is small.

The other systems which invite comparison are long braided rivers: these can remain statistically self-similar for long distances along and across the stream as a result of which boundary effects can be considered relatively unimportant.

One difficulty in making comparisons with the model is that since the simulation as described here conserves both water and sediment, it cannot produce areas of dry land from the initial conditions given. The solution adopted here was the comparatively crude one of taking a vertical displacement from the initial sediment plane and assigning each point as 'dry' or 'flooded' depending on whether it was higher or lower than the cut-off height.

Visual comparisons with photographs of real braided rivers [8–10] show a major difference: that the 'islands' of the simulation feature ragged edges with detail down to the lattice size (as suggested by the stability analysis) while the real ones are largely compact. Both, however, exhibit a power-law size distribution for the number of islands dN in a given range of area dA,

$$dN/dA \propto A^{-\gamma} \tag{13}$$

with the apparent exponent γ varying with the fraction of the channel that is underwater. These results are shown in figures 4 and 5 (figure 4 includes a sample plot from the simulation results). There is a well defined peak in the simulation values of the exponent, corresponding to an anisotropic percolation threshold; the spanning cluster predictably always crosses the grid along the direction of flow.

The considerable x-axis spread of the photograph data is due to the difficulty of defining properly the boundaries of the channel, and distinguishing large islands from part of the mainland. This problem is most noticeable at small water coverage (corresponding to channels near or below the percolation threshold in the model) where such debatable islands are a significant fraction of the exposed land within the channel. Comparison with the simulation also becomes more debatable at low water coverage since as less area is flooded, the approximation of simply 'draining' the simulation by a given amount and considering the exposed land, rather than removing the water as the landscape is evolving becomes cruder. Clearly the onset of percolation in a real river system is not well defined, since a truly spanning cluster would result in two separate rivers.

Nonetheless, while there is clearly a discrepancy, the measured exponents being less negative, they do not contradict the suggestion of a peak in the exponent at 40–45% water coverage, and these results do make the extension to other river systems appear worthwhile. One point being investigated with regard to the simulation is whether a

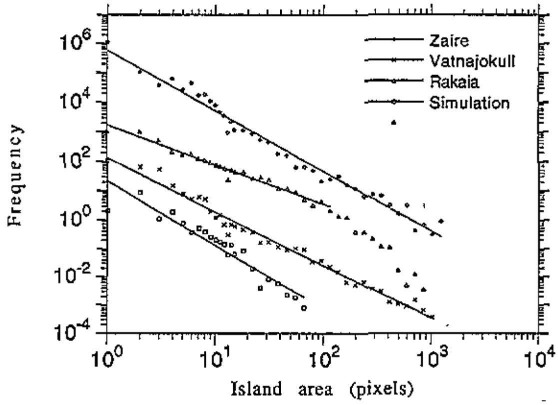

Figure 4. Island size distributions (simulation results correspond to 57% water cover).

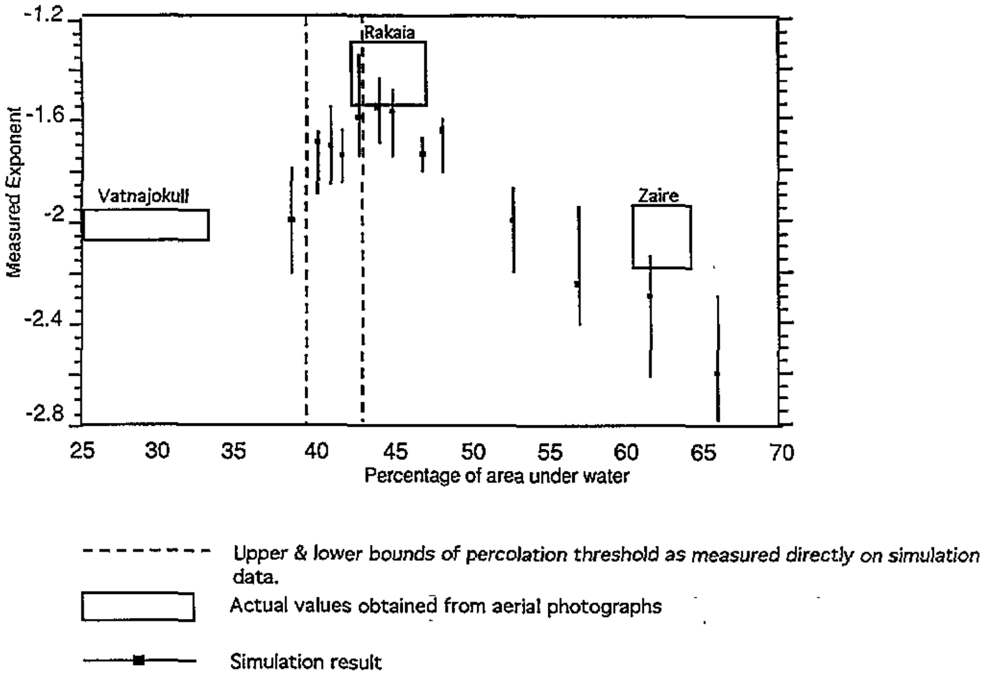

Figure 5. Apparent exponent as a function of water coverage.

simple convolution blurring of the deposition function to approximate turbulent mixing, which would remove the extreme small-scale detail of the simulated results, can give visually more realistic island patterns (it is also possible that this would make the apparent exponent less negative).

7. Conclusions and discussion

Our model has the minimal feature that water flows sensibly downhill as the landscape changes, and that water and sediment are conserved. This together with the simplest of erosion/deposition models appears sufficient to generate non-trivial landscape features of some realism.

The familiar formation of linear features oblique to the flow is supported by both analytic calculations of instability and also full numerical simulations. The correspondence between simulated landscape contours island size distributions in braided river systems is encouraging, although it may be the case that both are simply dominated by percolation statistics.

So far we have only studied the model under conditions where deposition and erosion are in overall balance: it is now important to examine what happens when one or the other has a net dominance. Various other details require further examination, particularly the role of the lattice cut-off in our simulations.

Acknowledgments

This project has been funded as a CASE project by BP in conjunction with SERC. Particular thanks to Drs Martin Blunt and Peter King at BP Research for their support and useful discussion and suggestions. Thanks also to Hans-Henrik Stoehlum for his suggestions and for providing the original references to the photographs used for analysis, and to Ian Robinson, for his valuable assistance in the image-processing required.

References

[1] Crane R C 1982 PhD thesis, Department of Geology. University of Reading
[2] Tetzlaff D M and Harbaugh J W 1989 *Simulating Clastic Sedimentation* (New York: Van Nostrand Reinhold)
[3] Cramer S and Marder M 1992 *Phys. Rev. Lett.* **68** 205
[4] Takayasu H and Inaoka H 1992 *Phys. Rev. Lett.* **68** 966
[5] Bak P, Tang C and Weisenfeld K 1987 *Phys. Rev. Lett.* **59** 381
[6] Allen J R L 1982 *Sedimentary Structures* vol 2 (Amsterdam: Elsevier)
[7] Komar P D 1976 *Beach Processes and Sedimentation* (New Jersey: Prentice-Hall)
[8] Summerfield M A 1991 *Global Geomorphology* (Harlow: Longman Scientific)
[9] Rust B R 1978 *Fluvial Sedimentology* Canadian Soc. Petr. Geol. Memoir 5
[10] Holmes A 1977 *Principles of Physical Geology* (Sunbury-on-Thames: Nelson)